The International Journal of Engineering and Science (IJES)
ISSN (e): 2319 – 1813 ISSN (p): 23-19 – 1805
|| Pages || PP 61-67 || 2020 ||

Evaporation of Water Droplets impacting upon heated surfaces

Rajeev Kumar Singh[1], Subrat Das[2], Peter D. Hodgson[3], Niladri Sen[4]
[1]*Research & Development Centre for Iron & Steel, Steel Authority of India Ltd, Ranchi-834002, India*
[2]*School of Engineering, Faculty of SEBE, Deakin University, Victoria-3217, Australia*
[3]*Office of Deputy Vice-Chancellor (Research), Deakin University, Victoria-3217, Australia*
[4]*Research & Development Centre for Iron & Steel, Steel Authority of India Ltd, Ranchi-834002, India*
Corresponding Author:singhrajeev@sail.in

----------***ABSTRACT***----------
A multiphase Volume of Fluid (VOF) model along with phase-change was developed to simulate evaporation and condensation of water droplets impacting upon a dry heated surface in the film evaporation regime. Simultaneous calculation of heat and mass transfer for the phase change during evaporation/condensation was modeled by coupling them through a mass flux model based on latent heat of vaporization of water and the pressure jump across the liquid interface (modified Schrage's model). To incorporate this coupling in the VOF model a User Defined Function in ANSYS FLUENT ® was written to analyze the growth of the vapor layer during evaporation. The developed mathematical model was used for a detailed analysis of the temporal evolution of the thermal gradients and fluid flow in and around the droplet in the film evaporation regime. It was found that vaporization starts from the advancing contact line. The contract front experiences the highest temperature gradient and localized heat transfer rate. The heat flux from the substrate to the droplet is directly proportional to the contact area of the droplet with the surface. Thus, higher heat flux can be achieved by better wetting of the surface by the droplet.

KEYWORDS: *-Droplet Evaporation, Volume of Fluid (VOF), Phase Change Model*

I. INTRODUCTION

Droplets evaporating from heated surfaces have found a wide range of industrial applications such as spray cooling[1], fire suppression systems[2], fuel injections[3], spray coating[4], inkjet printing[5]and likewise. This has generated substantial interest among the scientific community to pursue a fundamental analysis of heat, mass, and momentum transfer happening during evaporation. An idea into the relevance of this subject and the extent of interest in this area of research can be gathered from review articles on this subject[6]–[11]. Several physical phenomena associated with droplet evaporation that has been studied are depicted through a schematic in Figure 1.

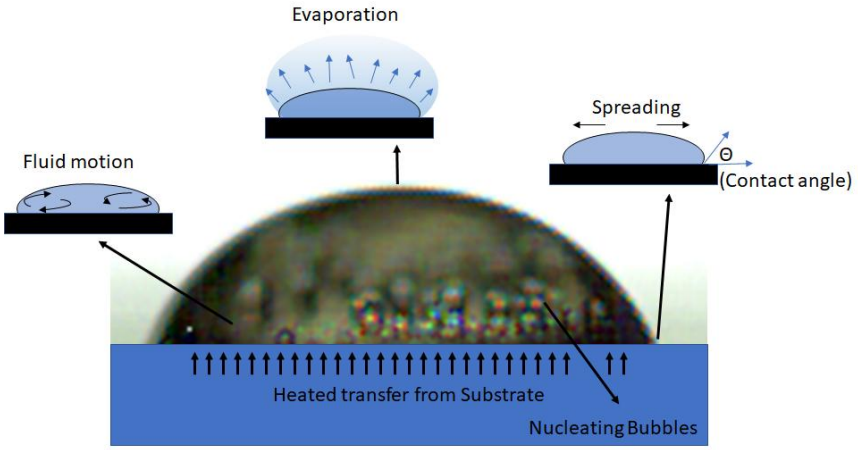

Fig. 1: Physics involved during droplet impact and evaporation from a heated surface

After the initial impact, the droplet first spreads on the heated surface and then retracts back while evaporating continuously. Thereafter, during its subsequent vaporization, the droplet exhibits very contrasting dynamic behavior with heat and mass transfer depending upon the degree of superheat($\Delta T = T_{droplet} - T_{surface}$). The droplet behavior on the surface is governed by three major groups of parameters, namely droplet properties such as its size, shape, and velocity; fluid properties such as density, viscosity,type of fluids such as

pure or multi-component; substrate properties such as surface roughness, inhomogeneity, temperature, and contact angle which the fluid subtends on the surface. These parameters can be clubbed together into well-known non-dimensional numbers such as Reynolds, Weber, Eckert, Bond, and Froude. Together, they lead to quite a different droplet behavior during its evaporation thus leading to varying heat transfer rates.

Surface temperature is known to have a significant influence on droplet behavior and leads to different mechanisms of heat transfer. Surface wetting characteristics also play a crucial role in modifying the droplet's impact dynamics and heat transfer phenomena[12]. The thermal properties of the substrate too are known to exert significant influence on the droplet heating behavior. For materials with high thermal conductivity, droplets tend to evaporate faster than that on substrates with low thermal conductivity[11]. The spread of the droplet, its contact angle hysteresis, the thickness of the vapor layer, and the droplet contact area on the surface are significantly influenced. Since spray cooling applications always involve surfaces with different textures (i.e. contact angle) and high temperatures, improved prediction of heat transfer rates at higher temperature demands an understanding of the influence of surface temperature and wetting characteristics on the spray cooling heat transfer rates.

A better understanding of the fundamental mechanism of heat transfer in spray cooling can be gathered from single droplet studies[11]. As it is experimentally difficult to control the interdependent parameters, it is much easier to analyze the behavior using numerical models[11]. In these numerical methods, the gas-liquid interface needs to be resolved to determine droplet shape during its interaction with the substrate.

Since evaporation occurs from the liquid-vapor interface, different numerical approaches for tracking the evaporating front have been employed. These methods are based on a fixed grid Eulerian method or moving grid Lagrangian methods or a combination of both. The location and shape of the interface are either tracked or captured using a separate indicator function. In the moving grid Lagrangian methods the mesh is moved or deformed to coincide with the free surface. These methods are very accurate but have limited applicability confined to cases where surface deformation is low or moderate. Finite Element-based Lagrangian[13], Boundary Fitted Coordinate[14]methods belong to this category of interface tracking method. In the fixed grid methods, the basic fluid flow is solved on fixed Eulerian grid and the interface is either tracked explicitly using marker points moving in Lagrangian fashion, e.g., Marker and Cell (MAC) method[15]or calculated implicitly from an indicator function like in Volume of Fluid[16]–[18] or Level Set Method[19]–[21] which are two popular interface capturing methods.In interface tracking methods, a separate set of mesh or marker points is overlaid on the underlying Eulerian grid and advected in Lagrangian fashion to track the droplet interface. The explicit tracking of droplet shape allows boundary conditions to be applied at the exact position. This can be useful for problems like that of evaporation where heat and mass transfer at the interface drives the physics of the problem. However, the need for usinga large number of marker points makes the simulation computationally expensive. On the other hand, in the interface capturing methods, model transport equations are solved as a single set of equations over the whole computational domain, and the interface is calculated by solving a separate transport equation for the scalar variable. The position of the interface is then derived from the value of this scalar field. This method is well suited for conditions where droplets may undergo large deformation or breakup. As the droplet shape is implicitly calculated, the computational mesh should be very fine to resolve the details. The fixed grid Eulerian methodshave wider applications as it can handle a wide variety of problems such as surfaces that undergo large deformation, breakup, or coalescence. Other methods such as Lattice Boltzmann Method[22], [23], Smooth Particle Hydrodynamics[24], Boundary Immersed Methods[25]too have been used for simulation of droplet heating and evaporation.Each of these techniques hasits advantages and disadvantages and there is no one universal method for simulation of droplet evaporation. The methodology of the formulation of these methods, their advantages and limitations have been detailed by Jafari and Ashgriz[26].

Of the various numerical techniques developed for modeling droplet evaporation on heated surfaces,the multiphase Volume of Fluid (VOF) model is most widely used. This is due to its advantage ofinherent mass conservation property and the ease in capturing the interface. The simple and efficient algorithm and ease of use make it popular for even complex problems that involve phase change across interface such as that arise due to evaporation/condensation in the film evaporation regime[18], [26]. The transport equations are solved in a fully Eulerian frame of reference. For a system having several phases, the mass or mole fraction of the individual phases in the cell is used to calculate the weighted average of the fluid and transport properties. The solution of the equations provides information only about the position of the interface in a particular cell through the volume fraction of individual phases in that cell. The interface face shape is then reconstructed using volume fraction information in that cell as well as that of a neighboring cell. Different interpolation schemes can be employed.

In the present work, the temporal evolution of fluid flow, the thermal field in and around the droplet along with vaporization at the liquid-vapor interface was studied using the VOF method. Spatial variation in the vaporization rates at the interface was computed using fluid properties as a function of local temperature. Since

it is difficult to visualize the formation of vapor, the work focuses on numerically simulating the effect of surface wetting characteristics (through the contact angle) and temperature on the droplet behavior during its interaction and evaporation from a heated surface. Emphasis is placed on the transitional period of droplet evaporation as significant variations in the fluid flow and heat transfer happens during this period. For this, a two-phase VOF model was used. As the default VOF method available in Ansys Fluent ® does not have a phase change model for film evaporation regime, User Defined Functions was developed to model phase change at the interface. The coupling between the heat and mass transfer was provided by using the model based on modified Schrage's equation[27]. The developed multiphase VOF model with phase change provided an insight into the heat transfer and evaporation from the droplet.

II. MATHEMATICAL MODEL

The mathematical model attempts to mimic the physics involved during the evaporation of a water droplet after it falls on a heated surface. Figure 2 shows the schematic of the computational representation along with the boundary conditions of a two-dimensional axisymmetric model of the droplet evaporation process from a heated substrate as depicted in Figure 1. A droplet of diameter (d_o) is allowed to impinge on a flat, dry and heated surface. The size of the computational domain ($M \times d_o, N \times d_o$) was taken large enough to prevent the flow near the boundariesto have any influence on the droplet'sspreading and evaporation behavior. A few initial simulations showed that $M = 10$ and $N = 5$were large enough to satisfy this criterion.The model considers the static contact angleas the time scale for the initial spreading behavior of the droplet is very small compared to the evaporation lifetime of the droplet. The gaseous mixture of water vapor and the air was considered as the primary phase and water was taken as the secondary phase. Temperature-dependent thermophysical properties of the water, air, and vapor were taken. Temperature-dependent surface tension was also considered.

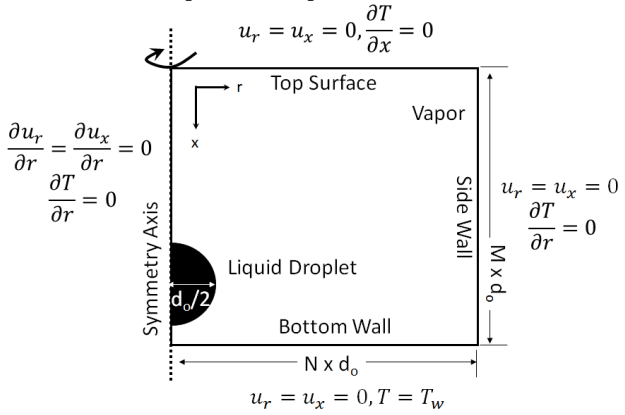

Fig. 2: Schematic of the 2D-axisymmetric simulation domain.

In the VOF model, similar in approach to that of Strotos et al. [28], tracking of the interface is carried by solving the transport equation for the volume fraction of water (secondary phase)[28]:

$$\frac{\partial \alpha_l}{\partial t} + \nabla.(\bar{u}\alpha_l) = \frac{-\dot{m}_{lg}}{\rho_l} \quad (1)$$

where $\alpha_l$is the volume fraction of the secondary phase (water), $\bar{u}$ is the velocity, ρ_l is the density of liquid and $\dot{m}_{lg}$ is the volumetric mass flux of evaporation from liquid to the gas phase ($kgm^{-3}s^{-1}$). The volume fraction of primary phase α_g is calculated from $\alpha_g = 1 - \alpha_l$.

For momentum balance, a single transport equation with weighted average transport properties is solved:[29]

$$\frac{\partial(\rho\bar{u})}{\partial t} + \nabla.(\rho\bar{u}\bar{u}) = -\nabla p + \nabla.[\mu(\nabla\bar{u} + \nabla\bar{u}^T)] + \rho g + F_\sigma \quad (2)$$

where g is the acceleration due to gravity and p pressure in the domain. The fluid properties of density and dynamic viscosity were taken as $\rho = \rho_l\alpha_l + \rho_g\alpha_g$and $\mu = \mu_l\alpha_l + \mu_g\alpha_g$respectively, whereas the surface tension force (F_σ)is converted into volume forces using the Continuum Surface Force (CSF) model proposed by Brackbill et al.[30]

$$F_\sigma = 2\sigma(\alpha_l\rho_l\kappa_l\nabla\alpha_l + \alpha_g\rho_g\kappa_g\nabla\alpha_g)/(\rho_l + \rho_g) \quad (3)$$

where κ is the curvature of the interface and given as divergence of unit normal $\hat{n}$ ADDIN ZOTERO_ITEM CSL_CITATION{"citationID": "TkxKpJJu", "properties": {"formattedCitation": "[29]", "plainCitation": "[29]", "noteIndex": 0}, "citationItems": [{"id": 3058, "uris": ["http://zotero. org/users /6754621/items/BE2XSNQ5"], "uri": ["http://zotero. org/users/6754621/items /BE2XSNQ5"], "itemData": {"id": 3058, "type": "article − journal", "page": "962", "source": "Zotero", "title": "Fluent Theory Guide", "author": [{"literal": "Ansys Inc.,

Southpointe, NY"}], "issued": {"date − parts": [["2019"]]}}}], "schema": "https://github. com/citation − style − language/schema/raw/master/csl − citation. json"} [29]

$$\kappa_l = -\kappa_g = -\nabla.\hat{n} \quad (4)$$

and$\hat{n} = \nabla\alpha_l/|\nabla\alpha_l|$is the normalized gradient of the liquid volume fraction.

The energy equation is expressed as:[29]

$$\frac{\partial(\rho h)}{\partial t} + \nabla.(\rho\bar{u}h) = \nabla.(\lambda\nabla T) - \dot{m}_{lg}L \quad (5)$$

where, L is latent heat of vaporisation (Jkg^{-1}), h is enthalpy(Jkg^{-1}), λ is thermal conductivity ($Wm^{-1}K^{-1}$) and T is the temperature (K)[29].

$$h = (\alpha_l\rho_l h_l + \alpha_g\rho_g h_g)/(\alpha_l\rho_l + \alpha_g\rho_g) \quad (6)$$

The enthalpy of the individual phases is calculated using the specific heat C_p with zero enthalpies at reference temperature (298.15 K)[29]

$$h_l = C_{p,l}(T - 298.15),\ h_g = C_{p,g}(T - 298.15) \quad \text{and } \lambda = \lambda_l\alpha_l + \lambda_g\alpha_g. \quad (7)$$

The mass transport of vapor species is solved using[28]:

$$\frac{\partial(\alpha_g\rho_g Y_{vap})}{\partial t} + \nabla.\left(\alpha_g\rho_g Y_{vap}\bar{u}\right) = \nabla.[\alpha_g\rho_g D\nabla Y_v] + \dot{m}_{lg} \quad (8)$$

where, Y_{vap} is the mass fraction of water vapor in the gas phase and D the diffusion coefficient of vapor species in air. When the water droplet touches the surface, wall adhesion accounted for the contact angle between the liquid and the surface and modified the surface normal as[29]:

$$\hat{n} = \hat{n}_w\ cos\ \theta\ +\ \hat{n}_t\ sin\ \theta \quad (9)$$

here, $\hat{n}_w$ and $\hat{n}_t$ are normal and tangential unit vectors to the wall, and θ contact angle between the liquid and the surface.

For phase change modeling the volumetric mass flux is calculated using the modified Schrage's equation and is modeled as[27]:

$$\dot{m}_{lg} = |\nabla\alpha|\left(\frac{2\beta}{2-\beta}\right)\left(\frac{MW}{2\pi RT}\right)^{0.5}\left(P_{sat} - P_{abs}X_{vap}\right) \quad (10)$$

Here, β is a model parameter called accommodation coefficient defining the probability of vapor molecules crossing the interface, MW is the molecular weight of water, R is the universal gas constant, P_{sat} is the saturation pressure of the vapor at temperature T at the interface, P_{abs} the absolute pressure in the domain and X_{vap}, the mole fraction of vapor in the gas phase at the interface.

The model assumes that the temperature of the interface and the vapor in its immediate neighborhood is at the same temperature and the driving force for mass transfer is the vapor pressure gradient across the interface. The phase change equation is enabled only on those computational cells which are intercepted by the interface. For this, the normalized gradient of volume fraction is used to mark the location of the interface cells.

The explicit VOF model assumes incompressible Newtonian fluids with laminar flow conditions. The pressure is calculated at the cell center using the PRESTO scheme while the pressure velocity equation is coupled using the PISO algorithm. The momentum, energy, and species equations were discretized using the second-order upwind differencing scheme. The unsteady terms were formulated using the first-order implicit method and solved using the Non-Iterative Time Advancement (NITA)[29] algorithm with variable time steps such that the Global Courant number never exceeded 0.1. Within each timestep, the solution was considered converged when the residual for continuity, momentum, and energy equation were all below 10^{-6}. This ensured accuracy in interface location. The shape of the interface was reconstructed using the Geo-Reconstruct Piecewise Linear Interpolating Scheme[29]. Though this scheme is computationally expensive than other schemes, nevertheless, it was used as it accurately locates and produces a sharp interface by calculating the linear shape of the interface within each cell based on the advection of fluid in each cell at each time step. The derivative and gradients employed in the model were computed using the Green-Gauss Node-based method with second-order accuracy.

III. RESULTS

The numerical model was validated as presented in a previous work published by the same group of authors[31]. The results presented here correspond to the simulation of a droplet of diameter 0.002m falling on a surface at 353 K. The impact Weber number was 1.3 and the Reynolds number was 440. The initial temperature of the droplet and the ambient was 293 K. Since the surface temperature was below the boiling temperature of the water, the heat transfer was in the film evaporation regime.

Figure 3 shows the shape of the droplet as it spreads on the surface and oscillates before it reaches its equilibrium position. In the first cycle of oscillation, during its spreading phase, vapor formation starts at the advancing contact line of the droplet. This region of the droplet experiences a very high-temperature gradient and the local heat transfer rate is highest at the contact front. As the droplet spreads further, the vapor cloud grows outward and upwards enclosing the droplet interface. During the receding stage, the droplet rises along

the central axis. The heated liquid near the contact line is drawn inwards, heating the bulk of the liquid. This is evident from the inward curling of the temperature contour lines which tend to ride along the droplet free surface. As the droplet recoils, heated fluid is drawn upwards and inwards. In the next cycle of spreading this heated fluid is once more spread on the surface, setting into motion a toroidal fluid flow in the droplet.

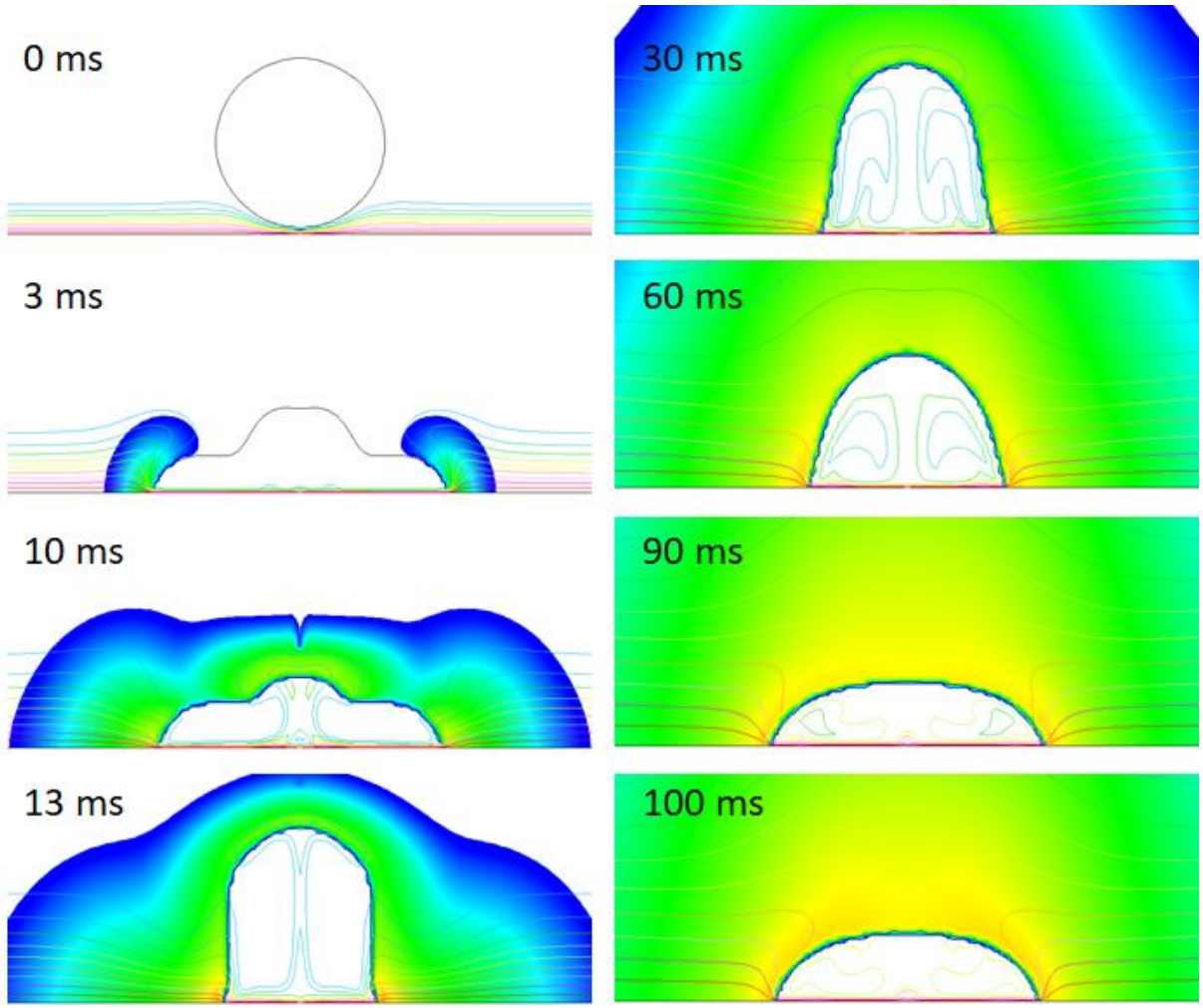

Fig. 3: Droplet shape and vapor contour during its evaporation ($T_{surface}$=353 K)

Figure 4 is a zoomed-in view of the droplet at 200ms along with the fluid flow vector profile and the thermal contours. At the center of the droplet, there is a formation of a stagnation zone which is at a higher temperature. The droplet is in its spreading phase. Along the central axis of the droplet, colder fluid is falling back towards the heated surface. On nearing the surface, this fluid moves outwards towards the contact line where due to the vapor movement the heated fluid is dragged upwards. This sets in the toroidal motion in the droplet. This periodic motion in the droplet continues till it keeps oscillating on the surface and a thermal gradient exists in the droplet.

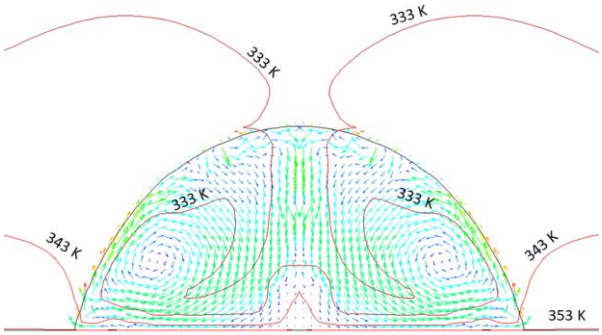

Fig.4: Fluid flow profile in the droplet at 200ms.

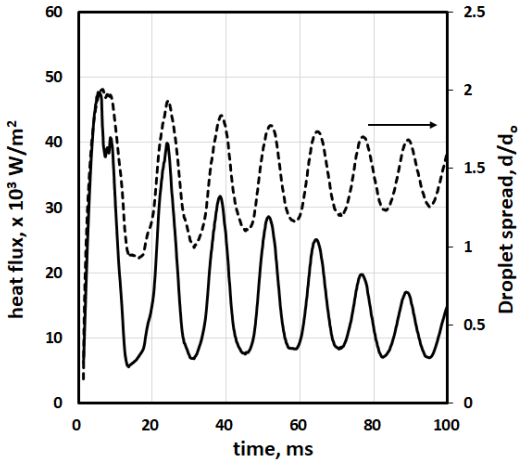

Fig.5: Temporal evolution of heat flux during droplet motion on the surface

Figure 5 shows the variation in heat transfer due to oscillation in the droplet. The dotted line depicts the non-dimensional drop spread (d/d_o) plotted against the time elapsed after impact. The solid line depicts the heat flux from the surface due to droplet motion. Initially, when the droplet contacts the surface, the temperature within the droplet is low, as the droplet spreads into a thin lamella creating a larger contact area with a high thermal gradient. This leads to increased heat flux with an increase in spread. As the droplet recedes the contact area reduces leading to the lowering of heat flux. The increase or decrease in heat flux from the surface is directly proportional to the increase or decrease in the contact area during oscillation. However, with elapse in time, the peak in heat flux with every spread is lowered. This may be attributed to the lowering of the thermal gradient in the drop as it gets heated up.

IV. CONCLUSION

A numerical model for simulation of droplet evaporation in the film evaporation regime has been developed. This model was used to characterize the vaporization behavior of an isolated drop falling on a heated surface. The local vaporization rate is highest near the contact line indicating that droplets vaporization predominantly at the contact front. Heat flux or the cooling effectiveness of the droplet is closely linked to its initial spreading behavior. Peak heat flux coincides with the maximum spreading diameter of the droplet. This suggests that higher impact velocity will lead to a higher evaporation rate as the droplet spread increases with increasing impact velocity. Higher impact velocity also leads to thinner film formation which leads to a larger thermal gradient across the film and hence increased heat transfer.

ACKNOWLEDGEMENTS

The authors thankfully acknowledge the permission of Deakin University, Australia, and Research and Development Centre for Iron & Steel (RDCIS), Steel Authority of India Ltd, India to present this paper. We also wish to acknowledge the support of all technical staff at Deakin University who have helped in sample preparation and setting up the experimental arrangement.

REFERENCES

[1] M. Dinc, "Computational Analysis of Single Drops and Sprays for Spray Cooling Applications," Doctoral Dissertation, West Virginia University, Morgantown, West Virginia, 2015.

[2] J. Floyd and R. McDermott, "Development and evaluation of two new droplet evaporation schemes for fire dynamics simulations," *Fire Saf. J.*, vol. 91, pp. 643–652, Jul. 2017, doi: 10.1016/j.firesaf.2017.04.036.

[3] S. S. Sazhin, W. A. Abdelghaffar, E. M. Sazhina, and M. R. Heikal, "Models for droplet transient heating: Effects on droplet evaporation, ignition, and break-up," *Int. J. Therm. Sci.*, vol. 44, no. 7, pp. 610–622, Jul. 2005, doi: 10.1016/j.ijthermalsci.2005.02.004.

[4] N. Espallargas, *Future Development of Thermal Spray Coatings*. Elsevier, 2015.

[5] H. Wijshoff, "Drop dynamics in the inkjet printing process," *Current Opinion in Colloid & Interface Science*, vol. 36, pp. 20–27, Jul. 2018, doi: 10.1016/j.cocis.2017.11.004.

[6] M. Rein, "Phenomena of liquid drop impact on solid and liquid surfaces," *Fluid Dyn. Res.*, vol. 12, no. 2, pp. 61–93, Aug. 1993, doi: 10.1016/0169-5983(93)90106-K.

[7] A. L. Yarin, "Drop Impact Dynamics: Splashing, Spreading, Receding, Bouncing…," *Annu. Rev. Fluid Mech.*, vol. 38, no. 1, pp. 159–192, Jan. 2006, doi: 10.1146/annurev.fluid.38.050304.092144.

[8] M. Marengo, C. Antonini, I. V. Roisman, and C. Tropea, "Drop collisions with simple and complex surfaces," *Current Opinion in Colloid & Interface Science*, vol. 16, no. 4, pp. 292–302, Aug. 2011, doi: 10.1016/j.cocis.2011.06.009.

[9] P. Cheng, X. Quan, S. Gong, X. Liu, and L. Yang, "Recent Analytical and Numerical Studies on Phase-Change Heat Transfer," in *Advances in Heat Transfer*, vol. 46, Elsevier, 2014, pp. 187–248.

[10] G. Liang and I. Mudawar, "Review of drop impact on heated walls," *Int. J. Heat Mass Transfer*, vol. 106, pp. 103–126, Mar. 2017, doi: 10.1016/j.ijheatmasstransfer.2016.10.031.

[11] D. Brutin and V. Starov, "Recent advances in droplet wetting and evaporation," *Chem. Soc. Rev.*, vol. 47, no. 2, pp. 558–585, 2018, doi: 10.1039/C6CS00902F.

[12] E.-S. R. Negeed, S. Hidaka, M. Kohno, and Y. Takata, "Effect of the surface roughness and oxidation layer on the dynamic behavior of micrometric single water droplets impacting onto heated surfaces," *Int. J. Therm. Sci.*, vol. 70, pp. 65–82, Aug. 2013, doi: 10.1016/j.ijthermalsci.2013.03.004.

[13] J. Fukai, Z. Zhao, D. Poulikakos, C. M. Megaridis, and O. Miyatake, "Modeling of the deformation of a liquid droplet impinging upon a flat surface," *Physics of Fluids A: Fluid Dynamics*, vol. 5, no. 11, pp. 2588–2599, Nov. 1993, doi: 10.1063/1.858724.

[14] C.-H. Kim, W. Zhang, and T. DebRoy, "Modeling of temperature field and solidified surface profile during gas–metal arc fillet welding," *Journal of Applied Physics*, vol. 94, no. 4, pp. 2667–2679, Aug. 2003, doi: 10.1063/1.1592012.

[15] F. H. Harlow and J. E. Welch, "Numerical Calculation of Time-Dependent Viscous Incompressible Flow of Fluid with Free Surface," *Phys. Fluids*, vol. 8, no. 12, p. 2182, 1965, doi: 10.1063/1.1761178.

[16] G. Strotos, I. Malgarinos, N. Nikolopoulos, and M. Gavaises, "Predicting the evaporation rate of stationary droplets with the VOF methodology for a wide range of ambient temperature conditions," *Int. J. Therm. Sci.*, vol. 109, pp. 253–262, Nov. 2016, doi: 10.1016/j.ijthermalsci.2016.06.022.

[17] A. M. Briones, J. S. Ervin, S. A. Putnam, L. W. Byrd, and L. Gschwender, "Micrometer-Sized Water Droplet Impingement Dynamics and Evaporation on a Flat Dry Surface," *Langmuir*, vol. 26, no. 16, pp. 13272–13286, Aug. 2010, doi: 10.1021/la101557p.

[18] D. Sun, J. Xu, and Q. Chen, "Modeling of the Evaporation and Condensation Phase-Change Problems with FLUENT," *Numer. Heat Transfer, Part B*, vol. 66, no. 4, pp. 326–342, Oct. 2014, doi: 10.1080/10407790.2014.915681.

[19] G. Son, "A level-set method for analysis of microdroplet evaporation on a heated surface," *J. Mech. Sci. Technol.*, vol. 24, no. 4, pp. 991–997, Apr. 2010, doi: 10.1007/s12206-010-0206-x.

[20] L. Rueda Villegas, R. Alis, M. Lepilliez, and S. Tanguy, "A Ghost Fluid/Level Set Method for boiling flows and liquid evaporation: Application to the Leidenfrost effect," *J. Comput. Phys.*, vol. 316, pp. 789–813, Jul. 2016, doi: 10.1016/j.jcp.2016.04.031.

[21] K. Luo, C. Shao, M. Chai, and J. Fan, "Level set method for atomization and evaporation simulations," *Progress in Energy and Combustion Science*, vol. 73, pp. 65–94, Jul. 2019, doi: 10.1016/j.pecs.2019.03.001.

[22] N. Karami, M. H. Rahimian, and M. Farhadzadeh, "Numerical simulation of droplet evaporation on a hot surface near Leidenfrost regime using multiphase lattice Boltzmann method," *Appl. Math. Comput.*, vol. 312, pp. 91–108, Nov. 2017, doi: 10.1016/j.amc.2017.05.038.

[23] E. Reyhanian, M. H. Rahimian, and S. FarshidChini, "Investigation of 2D drop evaporation on a smooth and homogeneous surface using Lattice Boltzmann method," *Int. Commun. Heat Mass Transfer*, vol. 89, pp. 64–72, Dec. 2017, doi: 10.1016/j.icheatmasstransfer.2017.09.019.

[24] X. Yang, M. Ray, S.-C. Kong, and C.-B. M. Kweon, "SPH simulation of fuel drop impact on heated surfaces," *Proceedings of the Combustion Institute*, vol. 37, no. 3, pp. 3279–3286, 2019, doi: 10.1016/j.proci.2018.07.078.

[25] G. Lupo, M. NiaziArdekani, L. Brandt, and C. Duwig, "An Immersed Boundary Method for flows with evaporating droplets," *International Journal of Heat and Mass Transfer*, vol. 143, p. 118563, Nov. 2019, doi: 10.1016/j.ijheatmasstransfer.2019.118563.

[26] A. Jafari and N. Ashgriz, "Numerical Techniques for Free Surface Flows: Interface Capturing and Interface Tracking," in *Encyclopedia of Microfluidics and Nanofluidics*, D. Li, Ed. Boston, MA: Springer US, 2014, pp. 1–27.

[27] R. W. Schrage, *A Theoretical Study of Interphase Mass Transfer*. Columbia University Press, 1953.

[28] G. Strotos, M. Gavaises, A. Theodorakakos, and G. Bergeles, "Numerical investigation on the evaporation of droplets depositing on heated surfaces at low Weber numbers," *Int. J. Heat Mass Transfer*, vol. 51, no. 7–8, pp. 1516–1529, Apr. 2008, doi: 10.1016/j.ijheatmasstransfer.2007.07.045.

[29] Ansys Inc., Southpointe, NY, "Fluent Theory Guide," p. 962, 2019.

[30] J. U. Brackbill, D. B. Kothe, and C. Zemach, "A continuum method for modeling surface tension," *J. Comput. Phys.*, vol. 100, no. 2, pp. 335–354, Jun. 1992, doi: 10.1016/0021-9991(92)90240-Y.

[31] R. K. Singh, S. Das, P. Hodgson, and N. Sen, "Droplet oscillation mechanism and its free surface behavior on impacting a heated hydrophobic surface at low Weber numbers," *Numer. Heat Transfer, Part A*, vol. 77, no. 1, pp. 13–32, Jan. 2020, doi: 10.1080/10407782.2019.1678957.